Journal of Volcanology and Geothermal Research 296 (2015) 31–39

Contents lists available at ScienceDirect

Journal of Volcanology and Geothermal Research

journal homepage: www.elsevier.com/locate/jvolgeores

Towards a quantitative understanding of pyroclastic flows: Effects of expansion on the dynamics of laboratory fluidized granular flows

L. Girolami [a,b,*], T.H. Druitt [a], O. Roche [a]

[a] Laboratoire Magmas et Volcans, Université Blaise Pascal – CNRS – IRD, OPGC, 5 rue Kessler, 63038 Clermont Ferrand, France
[b] Université François Rabelais de Tours, EA 6293 Géo-Hydrosystèmes Continentaux (GéHCO), Parc de Grandmont, 37200 Tours, France

ARTICLE INFO

Article history:
Received 15 November 2014
Accepted 5 March 2015
Available online 21 March 2015

Keywords:
Pyroclastic flows
Fluidized granular flows
Laboratory experiments
Scaling laws
Physical processes

ABSTRACT

We conducted laboratory dam-break experiments on initially fluidized granular flows using two different fine-grained powders (mean grain sizes 47 and 67 μm) down a smooth, horizontal channel with an impermeable base. The powders were first fluidized and expanded to a known degree in the flume reservoir, then released down the channel by opening a sliding gate. The mixture formed rapidly moving flows that defluidized and deposited progressively as they propagated. The experiments were similar to those carried out previously using volcanic ash by Girolami et al. (2008, 2010) but explored a much larger range of initial aspect ratios (height-to-length ratio, a = 0.25 to 4). They were designed to investigate the effects of initial expansion (up to 50 vol.% above loose packing) and aspect ratio on the dynamics of flow propagation and deposition, and to explore different scalings in order to determine the physical parameters governing these processes. The flows exhibit a similar behaviour to other types of transient granular flows, including three well defined propagation phases (acceleration, constant velocity, and stopping phases) and the progressive aggradation of a basal static layer during emplacement. The deposit aggradation velocity depends only on the initial powder expansion and is similar to that of a collapsing bed of the same powder, expanded by the same amount, under quasi-static, non-shearing conditions. At a given initial expansion, the maximum runout distance scales with the initial bed height h_0, the runout duration with $(h_0/g)^{1/2}$ and the maximum velocity with $(gh_0)^{1/2}$. However, runout distance and duration both increase with increasing initial expansion. This is attributed to the effect of hindered settling in delaying defluidization of the dense, but slightly expanded, suspension. The data enable us to identify an additive scaling law providing a smooth transition from non-expanded to expanded flows.

1. Introduction

Pyroclastic flows are a major hazard around volcanoes, and there is a need to develop quantitative models of their flow and sedimentation in order to make predictions of environmental and human impacts. Quantitative measurements of pyroclastic flows are commonly limited to frontal velocity (Levine and Kieffer, 1991; Loughlin et al., 2002) and acoustic or seismic signals (Calder et al., 2002; Ripepe et al., 2010); much of what we know about their physics is inferred qualitatively from deposits (e.g., Sparks, 1976; Branney and Kokelaar, 2002). Laboratory-scale experiments can play an important role in quantifying the physical processes operating during flow propagation, determining the dominant parameters governing the dynamics, and inferring scaling laws applicable to the natural systems.

In this paper, we focus on dense pyroclastic flows in which the particle concentration during transport is of the same order of magnitude as that in the final deposit. The broad spectrum of pyroclastic flow types range from short-lived, highly unsteady flows generated by lava dome collapse or by fallback of vulcanian eruption columns, to the quasi-steady ignimbrite-forming flows generated by sustained fountain collapses (Druitt, 1998; Branney and Kokelaar, 2002). The present paper concerns the dynamics of laboratory granular flows applicable to transient, unsteady pyroclastic flows of small volume (Girolami et al., 2008, 2010).

A large literature exists on the dynamics of transient 'dry' granular flows (i.e., those in which the effects of the interstitial fluid on the flow dynamics are negligible). Different experimental configurations (rectangular or axisymmetric) allow the slumping of a granular column and the abrupt release of grains across a horizontal surface (Balmforth and Kerswell, 2005; Lajeunesse et al., 2005; Lube et al., 2005; Mangeney-Castelnau et al., 2005; Lube et al., 2005). These different studies have resulted in a general understanding of such flows. Their behaviour is governed primarily by the initial aspect ratio of the column ($a = h_0/x_0$, where h_0 and x_0 are the reservoir height and length respectively) and not by the volume of material involved or the grain properties (size and shape). The flows exhibit three propagation phases: (1) a short initial acceleration phase, (2) a dominant constant-velocity phase, and (3) a brief stopping phase. They consist of a flowing layer above a

* Corresponding author at: Université François Rabelais, Laboratoire GéHCO, Parc Grandmont (Building E), Tours (France). Tel.: +33 0247367005; fax: +33 0247367090.
E-mail address: laurence.girolami@univ-tours.fr (L. Girolami).

http://dx.doi.org/10.1016/j.jvolgeores.2015.03.008
0377-0273/

basal static region that aggrades progressively with time until the flow is consumed and all motion ceases. Additional results, obtained from discrete element modelling simulations (Girolami et al., 2012; Wachs et al., 2010, 2012; Girolami et al., 2013), show that the dynamics of the three phases of transport is strongly dependant on the initial aspect ratio a. This parameter determines the ability of the column to convert potential energy to kinetic energy during the collapsing phase (Girolami et al., 2013). For a 2D channel geometry and initial aspect ratios less than about 2, only a superficial zone is involved in the flow (Girolami et al., 2013). The maximum runout distance scales mainly with the initial column height, so that $x_\infty - x_0 = K_x h_0$, where x_∞ is the runout and K_x is a constant. The initial geometry becomes important only at higher aspect ratios (Balmforth and Kerswell, 2005; Lajeunesse et al., 2005; Lube et al., 2005). Channel width and sidewall friction can also influence runout (Balmforth and Kerswell, 2005). The runout duration t_∞ scales with the gravitational free-fall time of the initial granular column: $t_\infty = K_t (h_0/g)^{1/2}$. The constants K_x and K_t depend on the material properties of the particles, such as the friction angle (Balmforth and Kerswell, 2005).

The ability of dense pyroclastic flows to travel long distances on slopes of only a few degrees has been attributed to friction reduction by non-equilibrium gas pore pressures and associated fluidization effects (Sparks, 1976; Wilson, 1980; Druitt et al., 2007; Girolami et al., 2008, 2010), so that studies of 'dry' granular flows are not strictly relevant. Fluidization is the process whereby a vertical gas flow passing through a granular bed generates an interstitial pore pressure that counteracts interparticle contact forces. This causes the granular material to take on liquid-like properties (Kunii and Lebenspiel, 1991; Rhodes, 1998). Roche and colleagues (2004, 2008) carried out dam-break experiments to investigate the effects of the interstitial gas on the dynamics of highly concentrated flows of fine (size <100 μm) glass beads. In their configuration the granular material was first fluidized under controlled conditions in a reservoir before release. The flows propagated down a horizontal channel with an impermeable base, allowing them to defluidize during emplacement. The gas-particle mixtures had a runout distance and runout time that scaled in the same way as for dry granular flows, and they exhibited the same three flow phases. In the predominant, constant-velocity, phase 2 the flow behaved as an inertial (i.e. inviscid) fluid with a frontal velocity $(gh_0)^{1/2}$ reflecting a balance between gravity and inertia (Roche et al., 2008). Further work showed that the flows defluidized through pore pressure diffusion and developed a basal static zone that accreted with time, so that deposition occurred progressively (Roche et al., 2010; Roche, 2012). In the experiments of Roche et al. (2004, 2008) the initial fluidized column of fine glass beads was expanded by no more than 8 vol.% above the loose packed state. However, experiments on poorly sorted, fine-grained volcanic ash (which forms the matrices of pyroclastic flows) have shown that this material can expand up to 45 vol.% when fluidized owing to the small particle size and low material permeability (Druitt et al., 2007).

Girolami et al. (2008) therefore carried out a similar series of dam-break experiments, but using initially fluidized volcanic ash capable of expanding up to 45 vol.% above the loose-packed state and, owing to its low permeability, of retaining gas pressure for longer than glass beads and hence causing longer flow runout at a given value of h_0. The ash was heated to 200 °C in order to reduce cohesive effects in the fine powder. The initially fluidized ash flows behave fundamentally like the glass-bead flows and thin progressively by deposition until they run out of volume. By using high-speed video imagery and a particle tracking algorithm, Girolami et al. (2010) showed that the upper surface of the deposit aggrades at a mean velocity identical to that inferred to take place at the base of a collapsing quasi-static bed of the same ash, expanded by the same initial amount, in the flume reservoir with the lock gate closed. Rapid shear apparently does not significantly influence the deposit aggradation rate beneath the flows of expanded ash under the conditions studied.

The present paper now extends the experiments of Girolami et al. (2008, 2010) on dense but expanded flows. The previous experiments on volcanic ash involved only a small range of initial column aspect ratios. In the present study we use two synthetic powders with different fluidization-expansion properties, as well as a larger range of aspect ratios. We compare their behaviour with that of the ash and explore explanations governing the propagation and sedimentation of dense, but slightly expanded, flows of fine-grained powders.

2. Fluidization concepts

A granular material is said to be fluidized when the drag force exerted by an upward interstitial flow of gas counterbalances the weight of the particles and generates interstitial pore fluid pressure, allowing the material to behave macroscopically in a manner analogous to a liquid (e.g., Kunii and Lebenspiel, 1991; Rhodes, 1998). Quasi-static (i.e., one-dimensional) beds of fine but cohesionless granular materials of mean grain size typically less than 100–200 μm (i.e. group A powders of Geldart's classification; Geldart, 1973) exhibit three regimes of fluidization according to the vertical superficial gas velocity imposed (V, gas volumetric flux divided by horizontal cross-section area): (1) an aerated regime in which V is less than the minimum fluidization velocity V_{mf} ($V < V_{mf}$); (2) a regime of uniform expansion in which $V_{mf} < V < V_{mb}$, where V_{mb} is the minimum bubbling velocity, and (3) a bubbling regime in which $V > V_{mb}$. If a fluidized group A powder is first uniformly expanded ($V_{mf} < V < V_{mb}$), then the gas supply is cut, pore pressure decreases through a diffusion process and the bed surface undergoes hindered settling at velocity V_{sett} which increases with the initial expansion, while a deposit aggrades from the base upwards at a velocity given by:

$$V_{agg} = V_{sett}/(E-1) \quad (1)$$

where $E = h_0/h_{mf}$, h_0 is the initial (expanded) bed height, and h_{mf} is the height at loose packing (i.e., at minimum fluidization velocity V_{mf}; e.g., Geldart, 1973; Lettieri et al., 2000; Druitt et al., 2007). The fractional expansion (fraction of excess gas) is equal to E-1.

Druitt et al.'s (2007) experiments showed that hot fluidized, poorly sorted sub-2 mm volcanic ash taken from the matrices of block-and-ash flow deposits and ignimbrites expanded significantly (up to 45 vol.%) prior to the onset of bubbling. Uniform expansion was greatest for fine-grained pyroclastic flow materials but decreased as coarser grain sizes were added. Our present experiments were therefore designed to evaluate the effects of initial uniform expansion on the dynamics of dam-break experimental flows of fluidized powders.

3. Experimental methods

The two powders, FCC and EZ, are industrial cracking catalysts used in the oil industry. FCC has a larger mean grain size (67 μm) than EZ (47 μm), and is better sorted (Table 1). Both powders are coarser and better sorted than the volcanic ash used in Girolami et al. (2008, 2010; Fig. 1, Table 1). FCC is non-cohesive and readily fluidizable at room temperature, whereas EZ is slightly cohesive and requires heating to expel atmospheric moisture before it can be fluidized. The EZ particles are more angular than the FCC ones. The maximum expansion possible in the non-bubbling state is larger for EZ (up to 50 vol.%) than for FCC (up to 25 vol.%). In some experiments, tracer particles of 500-μm silicon carbide were added in proportions up to a few vol%.

The experiments were carried out in a linear flume consisting of a rectangular fluidization reservoir (length 0.3 m, height 0.5 m, width 0.15 m), separated by a lock gate from a horizontal channel (length 3 m, height 0.3 m, width 0.15 m) built of aluminium and pyrex (Fig. 2). A metal partition enabled the material to be limited to a part of the reservoir, therefore reducing the effective reservoir length from 0.3 to 0.2 or 0.10 m. The reservoir and underlying windbox were heated

Table 1
Grain size analyses of the synthetic powders (EZ and FCC) determined by sieving at 0.5 phi intervals. Median and sorting parameters of Inman (1962). The volcanic ash of Girolami et al. (2008) is given for comparison.

Fraction (μm)	250–180	180–125	125–90	90–63	63–45	45–32	32–0	Median	Sorting
EZ	0.1	0.3	2.7	24.5	26.3	19.5	26.6	4.4	0.7
FCC	0.1	2	15.3	39.9	26.4	11.3	5.0	3.9	0.5
Ash	8.4	12.4	14.4	18.6	*46.2*[*]				

[*] <63 μm fraction.

externally by thermostat-regulated heating tapes, and all experiments were carried out with the incoming gas and reservoir contents at the same temperature. The granular material rested on a porous plate of mean pore size of 17 μm that separated the windbox from the reservoir. The gas flux entering the windbox was controlled by flow metres and was recalculated according to the operating temperature and the ideal gas law. The pressure drop across the bed was measured by a pressure transducer. The incoming gas could be directed either into the windbox

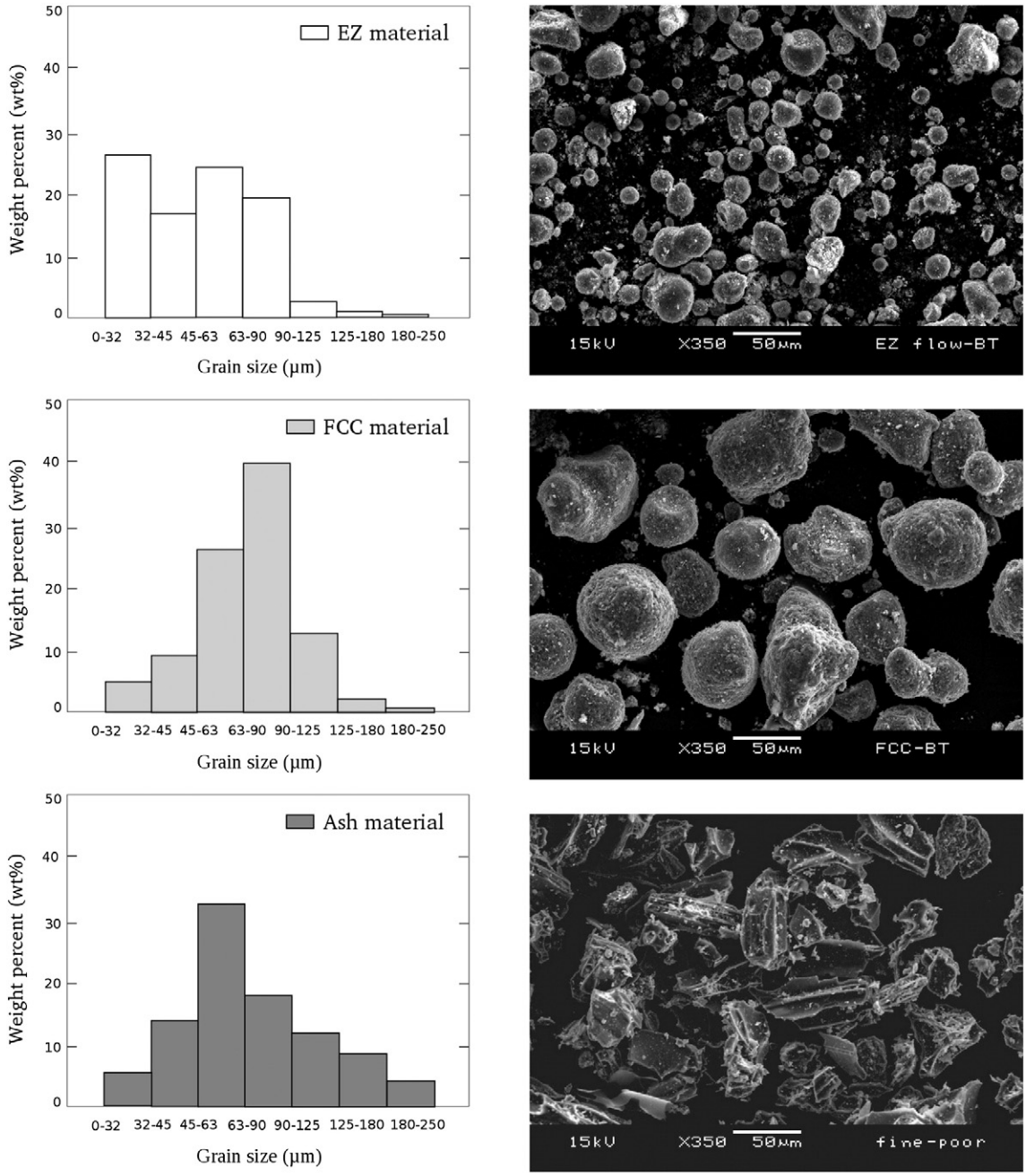

Fig. 1. Grain-size distributions and SEM images of the powders used (EZ, FCC and volcanic ash).

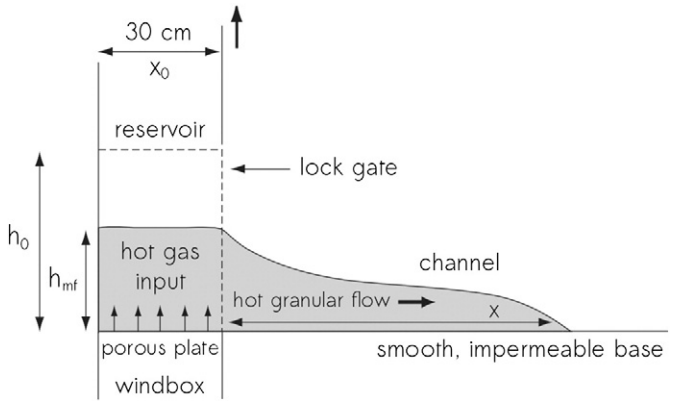

Fig. 2. Sketch of the laboratory flume used for experiments.

or vented outward during bed collapse tests as the gas supply was suddenly cut. The flume was described in detail by Girolami et al. (2008).

The powders were dried at 200 °C for 24 h prior to each experiment, then transferred as quickly as possible to the hot flume reservoir. The operating temperature of all experiments was fixed at 170 °C, which was high enough to avoid cohesive effects in the powders, especially EZ. All experiments were limited to the non-bubbling state (i.e. $V_{mf} < V < V_{mb}$), and the bed expansion was defined by $E = h_0/h_{mf}$ as in earlier works (Fig. 2).

Two procedures were followed for each powder.

1. *Quasi-static settling.* We studied the hindered settling behaviour of the two materials under quasi-static (non-shearing) conditions in bed-collapse tests performed in the reservoir of the apparatus with the gate shut. The bed was expanded to a known amount E, while stirring gently with a metal rod to avoid cohesion-induced gas channelling and to limit buildup of electrostatic charge (Druitt et al., 2007). The gas supply was then cut and the descent rate V_{sett} of the surface was measured. Five measurements were made for each expansion and the results were averaged. The sediment aggradation rate V_{agg} was calculated using Eq. (1) for each value of E. Cutting the gas supply trapped gas in the windbox, which was then vented upwards through the bed, such that quasi-static values of both V_{sett} and V_{agg} are underestimated (Park et al., 1991). However, this underestimation is at most around 10% which is comparable to the measurement error (Girolami et al., 2008).
2. *Flow generation.* Following the same procedure for expansion, the lock-gate was removed and the fluidized powders formed a fast-moving, short-lived, shear current that defluidized progressively during propagation until motion ceased. For each powder, two series of experiments were carried out: one (referred to hereon as 'variable-E') in which E was varied while keeping the non-expanded (i.e., minimum fluidization) height h_{mf} and reservoir length x_0 constant, and another (referred to hereon as 'constant-E') in which h_{mf} (and hence h_0) and x_0 were varied at constant E of 1.17. For each experiment, the entire flume was filmed at 25 frames per second to allow measurement of frontal velocity. The flow was also filmed at 30 cm from the lock gate for measurement of deposit aggradation rate. This was done by measuring the time interval Δt, at that location, between passage of the flow front and the end of deposition, as well as the final deposit thickness H. The mean value of V_{agg} was then given by H/Δt. This technique, also used by Girolami et al. (2008), assumed that (1) deposition is initiated immediately behind the flow front and (2) V_{agg} is constant with time. In fact, analysis of high-speed video footages has shown that deposition starts after a short time interval of ~0.1 s and that the aggradation rate actually increases slightly with time (see Fig. 9 of Girolami et al., 2010). Nevertheless, the difference between the observed aggradation rate and our estimated values of V_{agg} is negligible. Following each experiment, the deposit thickness was measured every 5 cm to construct the longitudinal profile.

Detailed sampling and size analysis, both vertically in the reservoir following procedure 1, and along the flume after procedure 2, revealed no significant particle segregation during expansion, flow or re-sedimentation of the powders. This enabled us to assign bulk properties to the powders and to interpret the results quantitatively.

4. Results

4.1. Quasi-static settling

For both powders, V_{mf} is approximately 0.1 cm/s, and V_{mb} is about ten times greater. The hindered settling functions $V_{sett}(E)$ for FCC and EZ are very similar to each other, as well as to that of the ash used by Girolami et al. (2008) (Fig. 3). Simple linear fits for this function are given in the caption of Fig. 3. Values of V_{agg} calculated using Eq. (1) ranged from 2 to 3.5 cm/s for the range of E studied.

4.2. Flow propagation and deposition

Results of the flow experiments are listed in Table 2. The flows emerged from the reservoir with thicknesses in the range 0.1–0.4 h_0. The flow-front motion exhibited the three phases typical of dam-break granular flows (Fig. 4). The initial gravitational acceleration phase lasted 0.1–0.2 s, and the stopping phase lasted 0.1–0.3 s. The intermediate constant-velocity phase accounted for 80% or more of the runout. Once the primary flow front had come to rest, a small wave of still-fluidized material approaching from behind broke (a few tenths of a second later) over the stationary front, extending the distal limit by up to 20 cm. This behaviour was also observed by Girolami et al. (2008). In what follows we restrict our attention to the primary flow wave and do not consider the limits of the secondary wave. The primary flow runout distance is termed x_∞, and the primary runout duration is termed t_∞. Distance x is measured from the rear of the reservoir (with the lock gate at $x = x_0$).

Runout distances $x_\infty - x_0$ ranged from 0.5 to 2.2 m, durations t_∞ ranged from 0.4 to 1.1 s, and maximum velocities ranged from 1.2 to 2.4 m/s. Fig. 4 shows the flow front position as a function of dimensionless runout distance and time, using the standard gravitational scalings for granular flows (Lajeunesse et al., 2005; Lube et al., 2005; Roche et al., 2008). Data for the variable-E experiments (Fig. 4a and c) show that the flow behaviours are sensitive to E, with both $x_\infty - x_0$ and t_∞ increasing with increasing E, as was also observed by Girolami et al. (2008) for

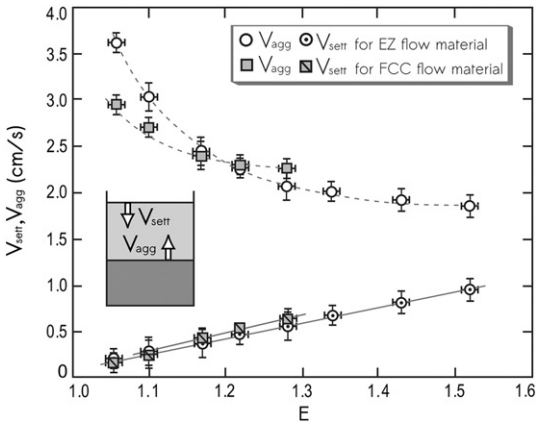

Fig. 3. Hindered settling (i.e. collapse of the bed surface) velocity and aggradation velocity of the basal deposit measured as a function of E during quasi-static bed collapse-tests performed in the lock reservoir. The trend-lines through the data are $V_{sett} = (E\text{-}0.932) / 0.604$ for EZ and $V_{sett} = (E\text{-}0.968) / 0.502$ for FCC. The values of V_{agg} are then given by Eq. (1).

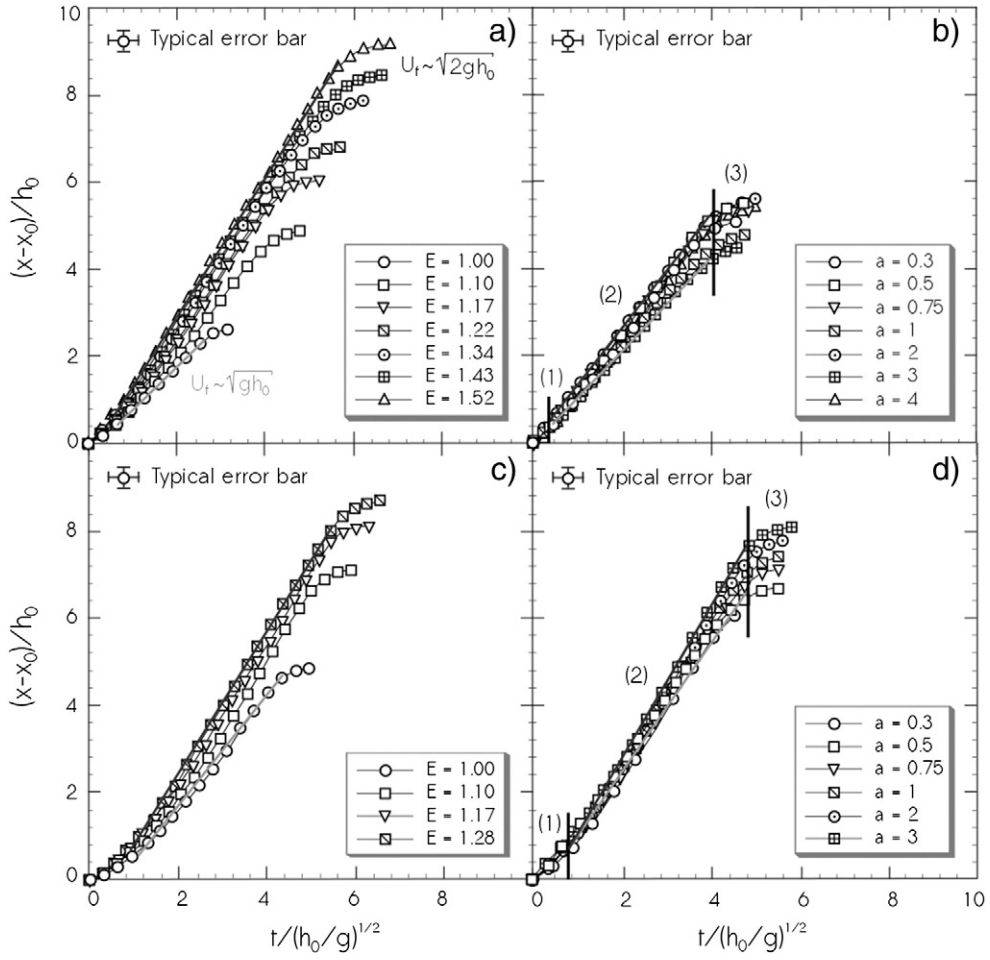

Fig. 4. (a) Front kinematic data plotted non-dimensionally using the scalings established for dry granular flows and fluidized flows of glass beads. (a) 'variable-E' data for EZ; (b) 'constant-E' (E = 1.17) data for EZ; (c) 'variable-E' data for FCC; (d) 'constant-E' data for FCC. For both materials, 'constant-E' data indicate the three well defined phases of transport (1), (2) and (3) separated by vertical black lines. The black and grey lines represent respectively the minimum and maximum frontal velocities, which scale with the characteristic velocity of dam-break flows.

volcanic ash. The maximum frontal velocity of most of the flows was $(2gh_0)^{1/2}$, this being the theoretical speed of an inviscid flow emerging from a slot (Roche et al., 2008). The lower velocities of the non-expanded flows (E = 1 flows of EZ and FCC) and one little-expanded flow (E = 1.1 flow of EZ) can probably be attributed to the effects of cohesive forces in both materials, and especially in EZ, which is slightly more cohesive than FCC, and/or energy dissipation through more frequent particle interactions owing to the higher particle concentration. The constant-E experiments (Fig. 4b and d) show that the initial aspect ratio $a = h_0/x_0$ has very little effect on flow behaviour. This in fact reflects an insensitivity to x_0 (the effect of h_0 being accounted for in the non-dimensionalization). An increase of x_0 of a factor of two

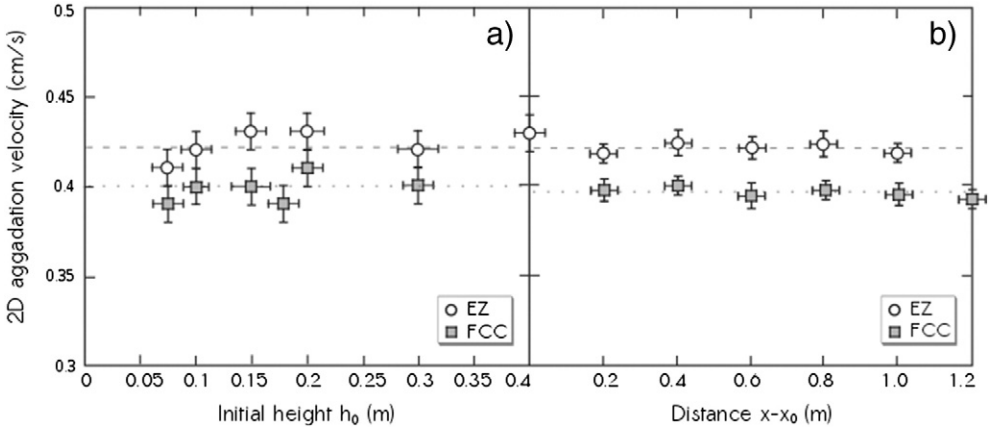

Fig. 5. Deposit aggradation velocity (V_{agg}) as a function of (a) initial bed height (h_0) and (b) distance from reservoir ($x–x_0$) for the 'constant-E' (E = 1.17) data involving both EZ Flow and FCC materials.

(at constant h_0 and E) decreases x_∞ and t_∞ by factors of only 0.8 and 0.95, respectively. The flow behaviour is governed almost entirely by h_0 and E within the range of aspect ratios studied ($a = 0.25 - 4.00$).

Deposition from the initially expanded flows was observed on high-speed video footages to take place by progressive aggradation of a basal static layer (Girolami et al., 2008, 2010). Fig. 5a and b shows measurements of sediment aggradation rate V_{agg} measured beneath flows of EZ and FCC expanded to 17% ($E = 1.17$). V_{agg} remained approximately constant with distance from the reservoir to at least 1.5 m from the lock gate, after which the flows became too thin for precise measurement (Fig. 5b). V_{agg} for each material does not vary with h_0 (and hence flow velocity) despite a large range of this parameter (Fig. 5a). Aggradation rate therefore depends only on the initial expansion E. Values of V_{agg} lie typically between 2 and 3 cm/s, an order of magnitude smaller than those measured beneath dry granular flows (12–16 cm/s, Lube et al., 2005; 16–19 cm/s, Roche et al., 2010). Moreover, V_{agg} was approximately equal to that beneath a quasi-static bed of the same material in the lock reservoir with the gate closed (comparing the flow values of Fig. 5 with the quasi-static values of Fig. 3 for $E = 1.17$), as also observed by Girolami et al. (2010) for their flows of volcanic ash.

The final deposits have thicknesses of less than 10 cm (most <5 cm), and extend up to 2.6 m from the lock gate. The aspect ratio of the deposits (mean thickness divided by length) correlates inversely with the initial aspect ratio $a = h_0/x_0$, reflecting the spreading process during flow (Fig. 6a and b). The taller and narrower the initial column, the longer and thinner the deposit.

5. Discussion

In a previous paper, we studied the effect of the initial expansion of gas-fluidized volcanic ash on the flow dynamics, for values of E ranging from 1.00 to 1.45, while the initial aspect ratio ($a = h_0/x_0$) varied little, from 0.58 to 0.83 (Girolami et al., 2008). Our new results include additional series of experiments performed with two different types of Group-A powders and with a much wider range of initial geometries that allow us to investigate the scaling relationships with more confidence.

We first plot the constant-E data in order to investigate the effect of initial bed geometry on flow behaviour. In Figs. 7a and b, the maximum runout $x_\infty - x_0$ is plotted against h_0, and runout duration t_∞ is plotted against the gravitational collapse time $(h_0/g)^{1/2}$ for the constant-E ($E = 1.17$) experiments. The plots show that these scalings provide a reasonable first-order fit to the data, and they confirm that x_0 (and hence $a = h_0/x_0$) has a negligible effect on the flow dynamics, at least up to $a \leq 4$. Our results confirm that both the runout and duration of the flows depend primarily on h_0, reflecting a conversion of potential energy to kinetic energy as discussed by Roche et al. (2008, 2011). Our results, along with earlier works, show that this is true at least for aspect ratios up to ~3–4 for initially aerated flows (Roche et al., 2008) and up to ~2 for 'dry' flows for which side-wall effects may be important (Lube et al., 2005).

Armed with this, we then use the variable-E data to examine the effects of E (Fig. 7c and d). We also include the ash-flow data from 18 experiments of Girolami et al. (2008). The three materials (EZ, FCC and ash) form three discrete, quasi-parallel trends on the plots. The two series of ash data collapse onto a single trend. Each of the three trends of variable-E data is linear to convex-upwards. The combination of Fig. 7a, b and c, d suggests that the scaling governing the flow behaviour takes the form:

$$\left(\frac{x_\infty - x_0}{h_0}\right) = A_x + \left(\frac{x_{xs}}{h_0}\right) \tag{2}$$

$$\left(\frac{t_\infty}{\sqrt{(h_0/g)}}\right) = A_t + \left(\frac{t_{xs}}{\sqrt{(h_0/g)}}\right) \tag{3}$$

where A_x and A_t are the dimensionless runout distance and time respectively of non-expanded mixtures ($E = 1$), x_{xs} is the excess runout distance and t_{xs} is the excess runout time. The additive nature of this law provides a smooth transition from non-expanded to expanded flows. The data of Fig. 7a, b and c, d suggest that t_{xs} and x_{xs} are principally functions of E. However the 'variable-E' series of experiments were carried out at constant h_{mf}, not constant h_0. As a result of this, and the minor scatter on Fig. 7a–d, we cannot rule out a weak dependence of t_{xs} and x_{xs} on h_0.

We propose that the key to understanding these data lies in the defluidization behaviour of expanded powders. The runout excess (x_{xs}, t_{xs}) can be attributed to the effects of initial expansion in prolonging gas retention in the flows. The larger the initial expansion, the greater the amount of gas that must escape for defluidization to be achieved. A conceptual basis for this can be understood by considering the behaviour of collapsing, *quasi-static* beds. Defluidization of a quasi-static bed of aerated ($V \leq V_{mf}$) powder occurs by the diffusion of pressure through the permeable (but non-expanded) particle framework. Defluidization of a quasi-static bed of an initially *expanded* powder ($V_{mf} < V < V_{mb}$) takes place, on the other hand, by two simultaneous processes (Druitt et al., 2007): (1) hindered settling of the expanded material, followed by (2) pressure diffusion from the aggrading, basal layer (i.e., deposit), with friction acquisition from the base upwards. Initial expansion increases the duration of pore pressure retention compared to the same bed non-expanded (Druitt et al., 2007; Montserrat et al., 2012; Roche, 2012). We therefore deduce that, at least conceptually,

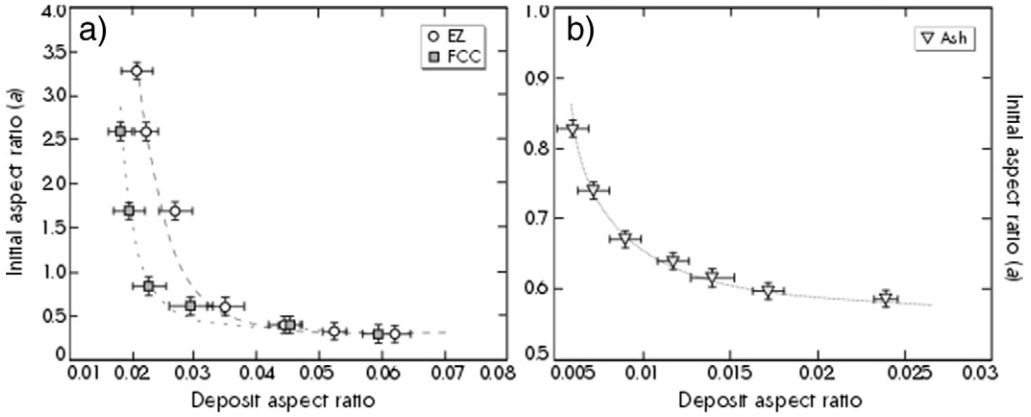

Fig. 6. Deposit aspect ratio (mean thickness/length) as a function of the initial aspect ratio for constant-E (FCC, EZ) and variable-E (ash) experiments.

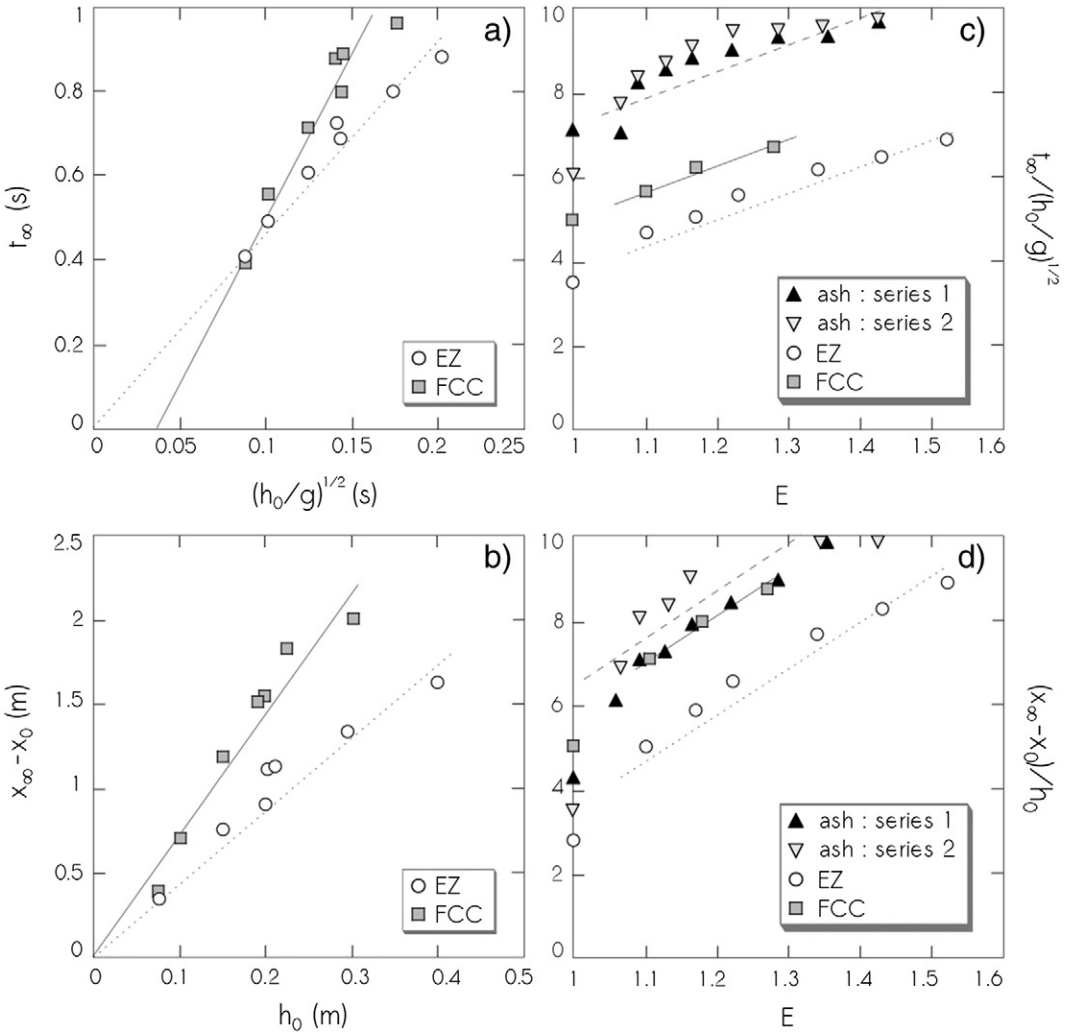

Fig. 7. (a, b) Scalings for the 'constant-E' experiments: runout time (t_∞) scales with the column free fall time $(h_0/g)^{1/2}$ while runout distance (x_∞–x_0) scales with the collapse height (h_0); (c, d) Scalings for the 'variable-E' experiments: non dimensional runouts as a function of E.

defluidization in initially-fluidized granular flows may take place in three modes:

- Dry ($V = 0$) granular flows have runouts governed by well established scaling laws involving gravity effects and the initial geometry of the column (Lajeunesse et al., 2005; Lube et al., 2005).
- Aerated (i.e., $E = 0$; $V < V_{mf}$) flows have runout exceeding those of dry granular flows due to the presence of interstitial gas pore pressure, which maintains reduced interparticle friction during the duration of flow runout until the pressure is totally released through diffusion (Roche et al., 2010; Roche, 2012).
- Uniformly fluidized (i.e., $E > 1$; $V_{mf} < V < U_{mb}$) flows have runouts that are enhanced both by (1) hindered settling in the expanded upper part of the flow, as well as (2) pore pressure diffusion in basal and/or distal parts of the flow in which the material has settled and is moving in a non-expanded, or little-expanded, state (Girolami et al., 2008, 2010).

As in our previous work on expanded flows of volcanic ash, the flows of FCC and EZ powders undergo hindered settling during transport. This is clear, because the deposit aggradation rates measured at the bases of the flows depend only on the initial expansion E and are the same as those in quasi-static collapsing beds of the same materials (see the discussion in Girolami et al., 2010). Based on these arguments, we interpret the additive law in Eqs. (2) and (3) as showing that the excess runout (x_{xs} and t_{xs}) of the expanded flows over aerated, but non-expanded, ones is due to excess gas retention time due to hindered settling. The more expanded the initial state of the flow, the longer the gas retention time and the further the runout.

In our first study of expanded granular flows (those using volcanic ash; Girolami et al., 2008) we tentatively proposed a scaling law for flow runout that involved two times characteristic of the system: $t_{grav} = (h_0/g)^{1/2}$, the gravitational acceleration timescale, and t_{sett}, a characteristic timescale governing quasi-static settling in the reservoir. We have tested this law with our present, much larger dataset, and have found that it does not adequately describe our new results. In particular, it lacks the additive character of Eqs. (2) and (3). We have also explored scaling laws of additive type relating t_{xs} and x_{xs} with t_{sett}, but have found no satisfactory fit to the data. In particular we plotted the data non-dimensionally as $(x_\infty - x_0) / x_0$ versus t_{sett} / t_{grav} and t_∞ / t_{grav} versus t_{sett} / t_{grav}, but the fit was not satisfying. While the evidence for an important role for hindered settling for flows of $E > 1$ is clear, it is complicated by the role of pressure diffusion in any basal, less expanded part of the flows. At this time no physically founded scaling law can be proposed to consistently predict the results.

Instead we explore a simple, empirical explanation for Eqs. (2) and (3). Let us assume that t_{xs} and x_{xs} are governed by the initial release

of excess height $h_0 - h_{mf}$ due to the expansion state of the mixture in reservoir. Since the frontal flow velocity scales with $(gh_0)^{1/2}$ (Fig. 4), the effect of this height excess is advected downstream at this speed. This reasoning suggests that $x_{xs} \propto (h_0 - h_{mf})$ and $t_{xs} \propto (h_0 - h_{mf})/\sqrt{gh_0}$, leading to the relationships:

$$\left(\frac{x_\infty - x_0}{h_0}\right) = A_x + B_x\left(\frac{E-1}{E}\right) \quad (4)$$

$$\left(\frac{t_\infty}{\sqrt{(h_0/g)}}\right) = A_t + B_t\left(\frac{E-1}{E}\right) \quad (5)$$

which are plotted on Fig. 8a and b. The resulting graphs strongly resemble those in Fig. 7b and d. The only points excluded from Fig. 7 are two experiments at the very lowest aspect ratios (0.25), which fall completely off the curves, and which are omitted from the plots.

As in our previous work on expanded flows of volcanic ash, the flows of FCC and EZ powders undergo hindered settling during transport. Moreover, the deposit aggradation rates measured at the bases of the flows depend only on the initial expansion E and are the same as those in quasi-static collapsing beds of the same materials (see the discussion in Girolami et al., 2010). Based on these arguments, we interpret the additive law in Eqs. (4) and (5) as showing that the excess runout (x_{xs} and t_{xs}) of the expanded flows over aerated, but non-expanded ones, is due to excess gas retention time and thus hindered settling. The more expanded the initial state of the flow, the longer the gas retention time and the further the runout. This explains why t_{xs} and x_{xs} are functions of E. Implicit in Eqs. (4) and (5) is that both non-expanded and expanded flows are governed by gravity, and that all processes and effects related to defluidization, sedimentation and pore-pressure diffusion (which depend on the intrinsic physical properties of each material; e.g., bed permeability and mixture elasticity), must be hidden in the constants B_x and B_t.

It is interesting that the data for the three different materials do not collapse onto a single line. Instead, they fall on lines with similar slopes, but different intercepts. The differences in mobility of the materials are therefore primarily due to differences in runout in the *non-expanded* state. Aerated ($E = 1$) flows of ash are systematically more mobile than aerated flows of EZ, whereas those of FCC have runout times similar to EZ but runout distances similar to ash. This may be related to the presence of higher proportions of fines in the ash (which tend to increase the bed ability for gas retention) than in the two synthetic powders. Increase in runout due to fines lubrication has been reported in granular flows (e.g. Phillips et al., 2006; Kokelaar et al., 2014). The angular shapes of the EZ particles may also be a factor.

6. Conclusions

This series of studies (Girolami et al., 2008, 2010; this paper) was conceived to investigate the role of expansion and progressive deposition in the propagation behaviour of laboratory flows of fine fluidized powders. It was motivated by the hypothesis that small-scale pyroclastic flows behave as large, shearing fluidized beds (Wilson, 1980; Roche et al., 2004; Druitt et al., 2007; Girolami et al., 2008, 2010). We carried out new experiments using two types of synthetic fine powder (EZ and FCC) with low permeabilities and low hindered settling rates. The experiments build on our previous experiments using volcanic ash, but involve a larger range of x_0 and initial aspect ratios. By combining the results with those of the volcanic ash, we have documented the effect of initial fluidization-generated expansion on flow behaviour, and have investigated possible scaling relationships governing the flows.

The difficulty in handling the slightly cohesive powders reduced the reproducibility and precision of the experiments compared to those involving fine (cohesionless) glass beads (e.g. Roche et al., 2008). Nevertheless, the flows have a similar behaviour to that previously documented for initially fluidized granular flows: (1) three propagation phases (acceleration, constant velocity, and deceleration), (2) a quasi-inviscid flow behaviour during the constant-velocity phase, (3) progressive deposition during flow runout, and (4) deposit aggradation rates similar to those beneath collapsing quasi-static beds of the same material at the same initial expansion.

Flow behaviour at a given initial expansion is governed by gravitational scaling laws very similar to those for non-expanded flows of cohesionless fluidized particles. The effect of initial aspect ratio is very small up to the largest value studied ($a = 4$). Other parameters being equal, both the runout distance and time increase with the degree of initial expansion of the powder. This expansion-dependence is attributed to the effect of slow hindered settling (due to low permeability) in delaying the defluidization of the dense, but weakly expanded, powder suspensions.

Acknowledgements

The authors wish to thank J.L. Fruquière for technical assistance throughout the project. This is Laboratory of Excellence ClerVolc contribution number 128.

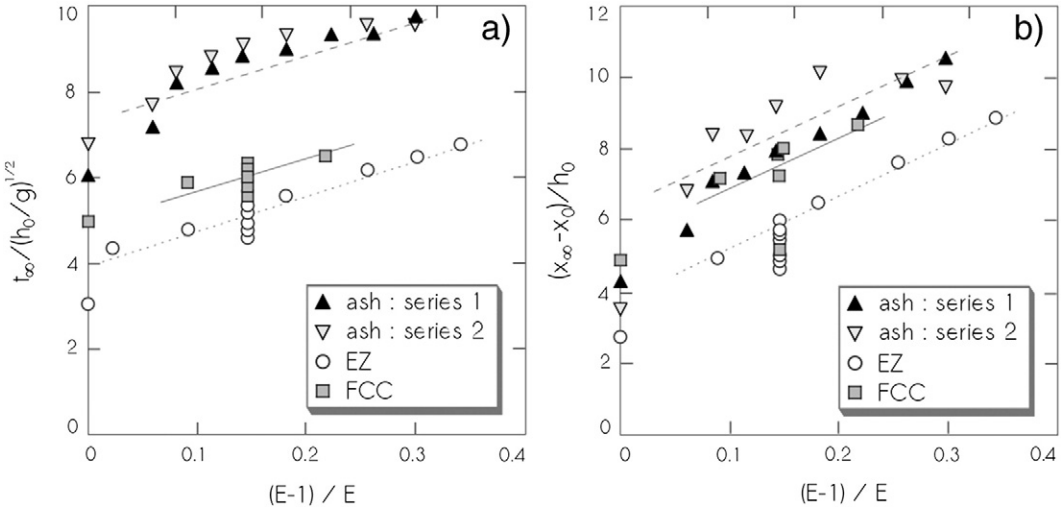

Fig. 8. (a, b) Runout time and distance plotted against (E-1)/E, based on a simple geometrical scaling (see discussion for details).

Table 2
Experimental results of this study and of Girolami et al. (2008).

Expt	E	h_0 (m)	x_0 (m)	h_0/x_0	$x-x_0$ (m)	t (s)
Powder EZ, variable E						
EZ	1.00	0.17	0.30	0.55	0.45	0.40
EZ	1.10	0.18	0.30	0.61	0.90	0.64
EZ	1.17	0.19	0.30	0.64	1.13	0.72
EZ	1.22	0.20	0.30	0.67	1.32	0.80
EZ	1.34	0.22	0.30	0.74	1.70	0.92
EZ	1.43	0.24	0.30	0.78	1.94	1.00
EZ	1.52	0.25	0.30	0.83	2.22	1.08
Powder EZ, constant E						
EZ	1.17	0.08	0.30	0.25	0.35	0.40
EZ	1.17	0.10	0.20	0.50	0.52	0.48
EZ	1.17	0.15	0.20	0.75	0.75	0.60
EZ	1.17	0.20	0.20	1.00	0.90	0.68
EZ	1.17	0.20	0.10	2.00	1.12	0.72
EZ	1.17	0.30	0.10	3.00	1.33	0.80
EZ	1.17	0.40	0.10	4.00	1.63	0.88
Powder FCC, variable E						
FCC	1.00	0.17	0.30	0.55	0.80	0.64
FCC	1.10	0.18	0.30	0.61	1.29	0.80
FCC	1.17	0.19	0.30	0.64	1.53	0.88
FCC	1.28	0.21	0.30	0.71	1.85	0.96
Powder FCC, constant E						
FCC	1.17	0.08	0.30	0.25	0.38	0.40
FCC	1.17	0.10	0.20	0.50	0.72	0.56
FCC	1.17	0.15	0.20	0.75	1.20	0.72
FCC	1.17	0.20	0.20	1.00	1.56	0.80
FCC	1.17	0.20	0.10	2.00	1.82	0.88
FCC	1.17	0.30	0.10	3.00	2.00	0.96
Volcanic ash Girolami et al. (2008; series 1)						
Ash	1.00	0.25	0.30	0.83	1.05	0.94
Ash	1.06	0.25	0.30	0.83	1.40	1.12
Ash	1.09	0.25	0.30	0.83	1.75	1.31
Ash	1.13	0.25	0.30	0.83	1.80	1.36
Ash	1.16	0.25	0.30	0.83	1.96	1.40
Ash	1.22	0.25	0.30	0.83	2.08	1.43
Ash	1.29	0.25	0.30	0.83	2.21	1.48
Ash	1.36	0.25	0.30	0.83	2.44	1.48
Ash	1.43	0.25	0.30	0.83	2.60	1.54
Volcanic ash Girolami et al. (2008; series 2)						
Ash	1.00	0.17	0.30	0.55	0.60	0.88
Ash	1.06	0.18	0.30	0.59	1.20	1.04
Ash	1.09	0.18	0.30	0.60	1.50	1.14
Ash	1.13	0.19	0.30	0.62	1.55	1.20
Ash	1.17	0.19	0.30	0.64	1.77	1.28
Ash	1.22	0.20	0.30	0.67	2.04	1.36
Ash	1.35	0.22	0.30	0.74	2.20	1.44
Ash	1.43	0.25	0.30	0.83	2.45	1.53

References

Balmforth, N.J., Kerswell, R.R., 2005. Granular collapse in two dimensions. J. Fluid Mech. 538, 399.

Branney, M.J., Kokelaar, P., 2002. Pyroclastic density currents and the sedimentation of ignimbrites. Geol. Soc. Lond. Mem. Lond. 27, 152.

Calder, E.S., Luckett, R., Sparks, R.S.J., Voight, B., 2002. Mechanisms of lava dome instability and generation of rockfalls and pyroclastic flows at Soufrière Hills Volcano, Montserrat. Geol. Soc. Lond. Mem. 21, 173–190.

Druitt, T.H., 1998. Pyroclastic density currents. Geol. Soc. Lond. Spec. Publ. 145, 145–182.

Druitt, T., Avard, G., Bruni, G., Lettieri, P., Maes, F., 2007. Gas retention in fine-grained pyroclastic flow materials at high temperatures. Bull. Volcanol. 69, 881–901.

Geldart, D., 1973. Types of gas fluidization. Powder Technol. 7, 285–292.

Girolami, L., Druitt, T.H., Roche, O., Khrabrykh, Z., 2008. Propagation and hindered settling of laboratory ash flows. J. Geophys. Res. 113, B02202. http://dx.doi.org/10.1029/2007JB005074.

Girolami, L., Roche, O., Druitt, T.H., 2010. Velocity fields and depositional processes in laboratory ash flows, with implications for the dynamics of dense pyroclastic flows. Bull. Volcanol. 72, 747–759. http://dx.doi.org/10.1007/s00445-010-0356-9.

Girolami, L., Hergault, V., Vinay, G., Wachs, A., 2012. A three-dimensional discrete-grain model for the simulation of dam-break rectangular collapses: comparison between numerical results and experiments. Granul. Matter 14 (3), 381–392.

Girolami, L., Wachs, A., Vinay, G., 2013. Unchannelized dam-break flows: effects of the lateral spreading on the flow dynamics. Phys. Fluids 25 (4), 043306.

Inman, D.L., 1962. Measures for describing the size distribution of sediments. J. Sediment. Petrol. 22, 125–145.

Kokelaar, B.P., Graham, R.L., Gray, J.M.N.T., Vallance, J.W., 2014. Fine-grained linings of leveed channels facilitate runout of granular flows. Earth Planet. Sci. Lett. 385, 172–180. http://dx.doi.org/10.1016/j.epsl.2013.10.043.

Kunii, D., Lebenspiel, O., 1991. Fluidization engineering. Butterworth-Heinemann (487 pp.).

Lajeunesse, E., Monnier, J.B., Homsy, M., 2005. Granular slumping on a horizontal surface. Phys. Fluids 17, 103302.

Lettieri, P., Yates, J., Newton, D., 2000. The influence of interparticleforces on the fluidization behavior of some industrial materials at hightemperature. Powder Technol. 110, 117–127.

Levine, A.H., Kieffer, S.W., 1991. Hydraulics of the August 7, 1980, pyroclastic flow at Mount St. Helens, Washington. Geology 19, 1121–1124.

Loughlin, S.C., Calder, E.S., Clarke, A.B., Cole, P.D., Luckett, R., Mangan, M., Pyle, D., Sparks, R.S.J., Voight, B., Watts, R.B., 2002. Pyroclastic flows and surges generated by the 25 June 1997 dome collapse, Soufriere Hills Volcano, Montserrat. In: Druitt, T.H., Kokelaar, B.P. (Eds.), The Eruption of Soufriere Hills Volcano, Montserrat From 1995 to 1999. Mem. Geol. Soc. London 21, pp. 191–210.

Lube, G., Huppert, H.E., Sparks, R.S.J., Freundt, A., 2005. Collapses of two-dimensional granular columns. Phys. Rev. 72, 041301.

Mangeney-Castelnau, A., Bouchut, F., Vilotte, J.P., Lajeunesse, E., Aubertin, A., Pirulli, M., 2005. On the use of Saint Venant equations to simulate the spreading of a granular mass. J. Geophys. Res. 110, B09103. http://dx.doi.org/10.1029/2004JB003161.

Montserrat, S., Tamburrino, A., Roche, O., Niño, Y., 2012. Pore fluid pressure diffusion in defluidizing granular columns. J. Geophys. Res. 117, F02034. http://dx.doi.org/10.1029/2011JF002164.

Park, J.J., Park, J.H., Chang, I.S., Kim, S.D., Choi, C.S., 1991. A new bed-collapsing technique for measuring the dense phase properties of gas-fluidized beds. Powder Technol. 66, 249–257.

Phillips, J.C., Hogg, A.J., Kerswell, R.R., Thomas, N.H., 2006. Enhanced mobility of granular mixtures of fine and coarse particles, Earth Planet. Sci. Lett. 246, 466–480.

Rhodes, M., 1998. Introduction to particle technology. John Wiley & Sons (320 pp.).

Ripepe, M., De Angelis, S., Lacanna, G., Voight, B., 2010. Observation of infrasonic and gravity waves at Soufrière Hills Volcano, Montserrat. Geophys. Res. Lett. 37, L00E14. http://dx.doi.org/10.1029/2010GL042557.

Roche, O., 2012. Depositional processes and gas pore pressure in pyroclastic flows: an experimental perspective. Bull. Volcanol. 74, 1807–1820. http://dx.doi.org/10.1007/s00445-012-0639-4.

Roche, O., Gilbertson, M.A., Phillips, J.C., Sparks, R.S.J., 2004. Experimental study of gas-fluidized granular flows with implications for pyroclastic flows emplacement. J. Geophys. Res. 109, B10201. http://dx.doi.org/10.1029/2003JB002916.

Roche, O., Montserrat, S., Niño, Y., Tamburrino, A., 2008. Experimental observations of water-like behaviour of initially fluidized, unsteady dense granular flows and their relevance for the propagation of pyroclastic flows. J. Geophys. Res. 113, B12203. http://dx.doi.org/10.1029/2008JB 005664.

Roche, O., Montserrat, S., Niño, Y., Tamburrino, A., 2010. Pore fluid pressure and internal kinematics of gravitational laboratory air-particle flows: insights into the emplacement dynamics of pyroclastic flows. J. Geophys. Res. 115, B09206. http://dx.doi.org/10.1029/2009JB007133.

Roche, O., Atalli, M., Mangeney, A., Lucas, A., 2011. On the run-out distance of geophysical gravitational flows: insight from fluidized granular collapse experiments. Earth Planet. Sci. Lett. 311, 375–385. http://dx.doi.org/10.1016/j.epsl.2011.09.023.

Sparks, R.S.J., 1976. Grain size variations in ignimbrites and implications for the transport of pyroclastic flows. Sedimentology 23, 147–188.

Wachs, A., Vinay, G., Ferrer, G., Kouakou, J., Dan, C., Girolami, L., 2010. PeliGRIFF: a parallel DEM-DLM/FD method for DNS of particulate flows with collisions. Int. J. Mech. Syst. Sci. Eng. 1 (4), 185–191.

Wachs, A., Girolami, L., Vinay, G., Ferrer, G., 2012. GRAINS3D, a flexible DEM approach for particles of arbitrary convex shape — part I: numerical model and validations. Powder Technol. http://dx.doi.org/10.1016/j.powtec.2012.03.023.

Wilson, C.J.N., 1980. The role of fluidization in the emplacement of pyroclastic flows: an experimental approach. J. Volcanol. Geotherm. Res. 8, 231–249.